The Astrophysical Journal Letters, 755:L25 (7pp), 2012 August 20 doi:10.1088/2041-8205/755/2/L25

THE APACHE POINT OBSERVATORY GALACTIC EVOLUTION EXPERIMENT: FIRST DETECTION OF HIGH-VELOCITY MILKY WAY BAR STARS

David L. Nidever[1], Gail Zasowski[1], Steven R. Majewski[1], Jonathan Bird[2], Annie C. Robin[3], Inma Martinez-Valpuesta[4], Rachael L. Beaton[1], Ralph Schönrich[2], Mathias Schultheis[3], John C. Wilson[1], Michael F. Skrutskie[1], Robert W. O'Connell[1], Matthew Shetrone[5], Ricardo P. Schiavon[6], Jennifer A. Johnson[2], Benjamin Weiner[7], Ortwin Gerhard[4], Donald P. Schneider[8], Carlos Allende Prieto[9], Kris Sellgren[2], Dmitry Bizyaev[10], Howard Brewington[10], Jon Brinkmann[10], Daniel J. Eisenstein[11], Peter M. Frinchaboy[12], Ana Elia García Pérez[1], Jon Holtzman[13], Fred R. Hearty[1], Elena Malanushenko[10], Viktor Malanushenko[10], Demitri Muna[14], Daniel Oravetz[10], Kaike Pan[10], Audrey Simmons[10], Stephanie Snedden[10], and Benjamin A. Weaver[14]
[1] Department of Astronomy, University of Virginia, Charlottesville, VA 22904-4325, USA; dln5q@virginia.edu
[2] Department of Astronomy and the Center for Cosmology and Astro-Particle Physics, The Ohio State University, Columbus, OH 43210, USA
[3] Institut Utinam, CNRS UMR 6213, OSU THETA, Université de Franche-Comté, 41bis avenue de l'Observatoire, F-25000 Besançon, France
[4] Max-Planck-Institut für Extraterrestrische Physik, Giessenbachstrasse, D-85748 Garching, Germany
[5] McDonald Observatory, University of Texas at Austin, Fort Davis, TX 79734, USA
[6] Gemini Observatory, 670 North A'Ohoku Place, Hilo, HI 96720, USA
[7] Steward Observatory, 933 North Cherry Street, University of Arizona, Tucson, AZ 85721, USA
[8] Department of Astronomy and Astrophysics, The Pennsylvania State University, University Park, PA 16802, USA
[9] Instituto de Astrofísica de Canarias, E-38205 La Laguna, Tenerife, Spain
[10] Apache Point Observatory, Sunspot, NM 88349, USA
[11] Harvard-Smithsonian Center for Astrophysics, 60 Garden Street, MS 20, Cambridge, MA 02138, USA
[12] Department of Physics and Astronomy, Texas Christian University, Fort Worth, TX 76129, USA
[13] Department of Astronomy, New Mexico State University, Las Cruces, NM 88003, USA
[14] Center for Cosmology and Particle Physics, New York University, New York, NY 10003, USA
Received 2012 June 22; accepted 2012 July 12; published 2012 July 31

ABSTRACT

Commissioning observations with the Apache Point Observatory Galactic Evolution Experiment (APOGEE), part of the Sloan Digital Sky Survey III, have produced radial velocities (RVs) for ∼4700 K/M-giant stars in the Milky Way (MW) bulge. These high-resolution ($R \sim 22{,}500$), high-S/N (>100 per resolution element), near-infrared (NIR; 1.51–1.70 μm) spectra provide accurate RVs ($\epsilon_V \sim 0.2$ km s^{-1}) for the sample of stars in 18 Galactic bulge fields spanning $-1^\circ < l < 20^\circ$, $|b| < 20^\circ$, and $\delta > -32^\circ$. This represents the largest NIR high-resolution spectroscopic sample of giant stars ever assembled in this region of the Galaxy. A cold ($\sigma_V \sim 30$ km s^{-1}), high-velocity peak ($V_{GSR} \approx +200$ km s^{-1}) is found to comprise a significant fraction (∼10%) of stars in many of these fields. These high RVs have not been detected in previous MW surveys and are not expected for a simple, circularly rotating disk. Preliminary distance estimates rule out an origin from the background Sagittarius tidal stream or a new stream in the MW disk. Comparison to various Galactic models suggests that these high RVs are best explained by stars in orbits of the Galactic bar potential, although some observational features remain unexplained.

Key words: Galaxy: bulge – Galaxy: kinematics and dynamics – Galaxy: structure – surveys

Online-only material: color figures

1. INTRODUCTION

Multiple *N*-body models have demonstrated that rotating stellar disks form bars relatively quickly under a wide variety of conditions (e.g., Bureau & Athanassoula 2005; Debattista et al. 2006; Martinez-Valpuesta et al. 2006), and observations have identified a high incidence of large central bars in extragalactic systems (e.g., Lütticke et al. 2000; Chung & Bureau 2004). Even in edge-on spiral galaxies, where the stellar bar can be difficult to isolate photometrically from the surrounding bulge and/or disk, the bar can be identified via kinematical signatures: double-peaked rotation curves, radial velocity (RV) dispersion profiles with particular combinations of plateaus and peaks/minima, and the relation between the mean and higher moments of the RV distribution (e.g., Bureau & Athanassoula 2005).

In recent decades, good evidence for a Milky Way (MW) bar has arisen from infrared (IR) surface brightness maps and star counts (e.g., Blitz & Spergel 1991; Weinberg 1992; Dwek et al. 1995; Hammersley et al. 2000; Cole & Weinberg 2002; Benjamin et al. 2005; López-Corredoira et al. 2007; Rattenbury et al. 2007; Robin et al. 2012), carbon stars (Cole & Weinberg 2002), the solar neighborhood velocity field (e.g., Dehnen 2000; Minchev et al. 2007), microlensing (e.g., Gyuk 1999), and inner Galaxy *gas* kinematics (e.g., Liszt & Burton 1980; Binney et al. 1991; Fux 1999; Weiner & Sellwood 1999). However, the high extinction toward the inner Galaxy midplane ($A_V \approx 5$–10) has long precluded an extensive spectroscopic survey of the type required to measure the bulge/bar *stellar* kinematics on par with studies of extragalactic bars in galaxies viewed edge-on.

More recently, the BRAVA (Rich et al. 2007) and ARGOS (Ness & Freeman 2012) surveys have begun performing kinematical measurements in the bulge periphery, mapping the bulk cylindrical (i.e., bar-like) rotation of the bulge. In this Letter, we report the discovery, within data from the new APOGEE survey, of a "cold" kinematical feature in the inner disk, which has not been seen in previous surveys and is, most likely, a signature of particular stellar orbits in the MW bar. In Section 2,

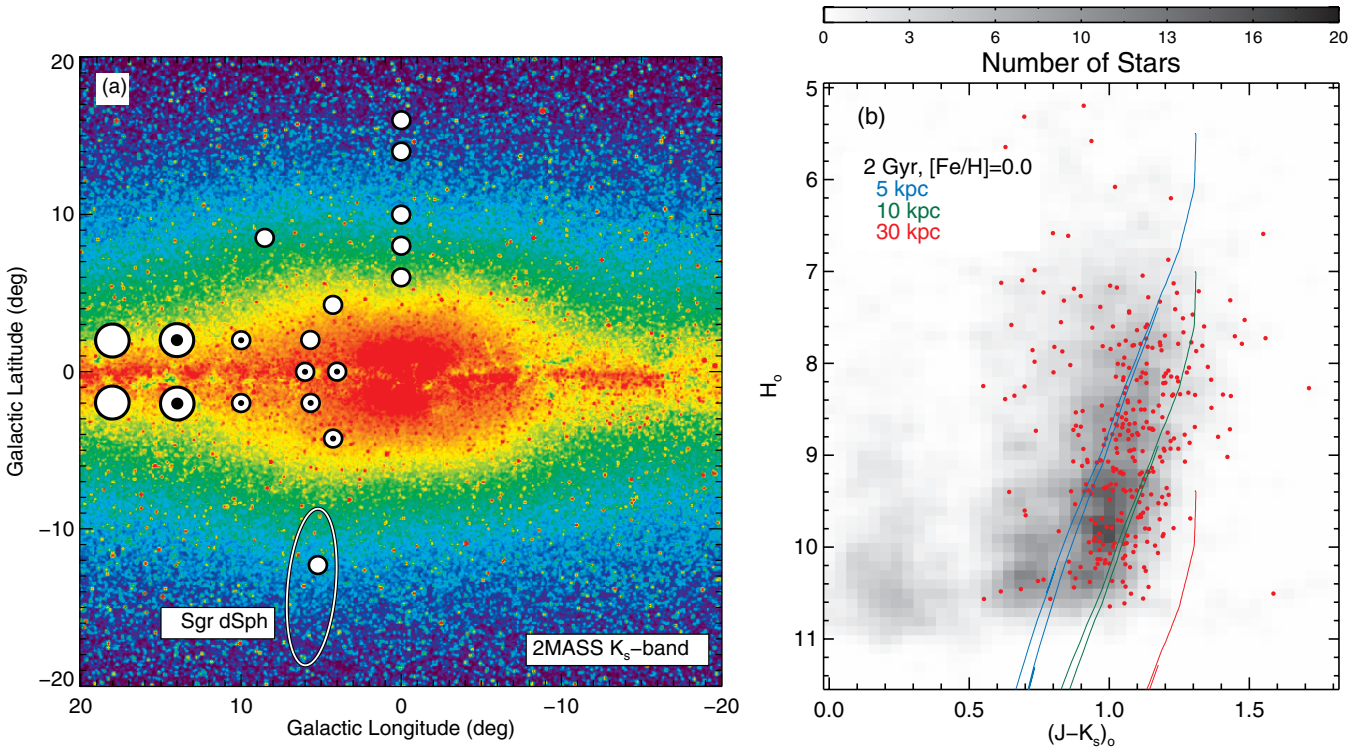

Figure 1. (a) Coverage of APOGEE commissioning fields (white circles) in the Galactic bulge and inner disk regions. The eight fields with distinct high-velocity peaks are marked with black dots. The background image is the 2MASS K_s band (Skrutskie et al. 2006) showing the boxy bulge. The Sagittarius dwarf spheroidal is indicated by an ellipse. (b) Reddening-corrected Hess diagram of all observed stars (gray scale) with the high-velocity stars with $[J - K_s]_0 \geqslant 0.5$ shown as red dots. The high-velocity thresholds in Table 1, which represent the RV of the "trough" between the main peak and the high-velocity peak, were used to select the high-velocity stars from each field. Fiducial Girardi et al. (2002) isochrones (2 Gyr, [Fe/H] = 0.0) are shown at distances of 5/10/30 kpc (blue/green/red).

(A color version of this figure is available in the online journal.)

we briefly describe the observations and data reduction, and we present in Section 3 the RV distributions of the APOGEE fields, along with the RV predictions of multiple Galactic kinematical models. In Section 4, we use these comparisons to interpret the nature of the APOGEE observations, and we evaluate alternative explanations for the data and model discrepancies.

2. OBSERVATIONS AND DATA REDUCTION

The APOGEE project (Eisenstein et al. 2011; S. R. Majewski et al., in preparation) uses a custom-built, cryogenic spectrograph (Wilson et al. 2010) recording 300 simultaneous near-IR spectra (1.51–1.70 μm) fed from the Sloan 2.5 m telescope (Gunn et al. 2006). The final configuration for the spectrograph is described in J. C. Wilson et al. (in preparation); however, the data described here were taken before the instrument was in its fully commissioned state and in optimal focus (achieved 2011 September). The net effect was a somewhat blurred line-spread function, yielding a degradation of the resolution primarily in the red detector to $R \sim 16{,}000$ (1.65–1.70 μm) compared to $R \sim 23{,}000$ in the other two detectors (1.51–1.58 μm and 1.59–1.64 μm).

The APOGEE fibers are plugged into standard Sloan 2.5 m plugplates and observed similarly to those of the optical Sloan spectrographs, with the following variations: (1) 35 fibers in each plugplate configuration collect sky spectra, (2) another 35 fibers are placed on bright, hot stars to gauge telluric (CO_2, H_2O, and CH_4) absorption, and (3) because the large zenith distances required to observe the bulge from APO cause strong differential refraction, the field diameter was restricted to 1° for $l \lesssim 12°$ fields (2° for the rest).

We observed 18 bulge fields in 2011 June and July with $-1° < l < 20°$, $|b| < 20°$, and $\delta > -32°$ (see Figure 1(a)). Targets were selected from the Two Micron All Sky Survey (2MASS) Point Source Catalog (Skrutskie et al. 2006) requiring $(J - K_s)_0 \geqslant 0.5$ (although some plugplates had no color selection for testing purposes) and $H \leqslant 11.0$ (see G. Zasowski et al., in preparation, for details on APOGEE targeting strategy).[15] The dereddened Hess diagram for all observed stars is shown in Figure 1(b). Each field was observed for a total integration of roughly one hour, for a S/N > 100 per APOGEE pixel for each star.

An automated data reduction pipeline written specifically for APOGEE data (D. L. Nidever et al., in preparation) was used for (1) collapsing the sample-up-the-ramp datacubes to two-dimensional images with rejection of cosmic rays, (2) extraction of one-dimensional spectra from the two-dimensional images, (3) wavelength calibration using ThArNe/UrNe arc lamp exposures and airglow lines, (4) correction of telluric absorption as monitored by the 35 hot star standards, (5) subtraction of airglow lines and sky continuum, and (6) derivation of RVs by cross-correlation against a grid of template spectra spanning the expected range of temperatures, gravities, and metallicities of target stars. The median RV scatter for stars observed multiple times is 0.22 km s^{-1} (with a mode of ~0.09 km s^{-1}), while tests of derived RVs for observations of 53 stars in three globular clusters (M3, M13, and M15) with accurate literature RVs suggest that the zero point of the APOGEE pipeline RVs is accurate to $\sim 0.26 \pm 0.22$ km s^{-1}.

[15] The 2MASS photometry was dereddened using the RJCE method (Majewski et al. 2011), with *WISE* (Wright et al. 2010) and GLIMPSE (Churchwell et al. 2009) providing the required mid-IR photometry.

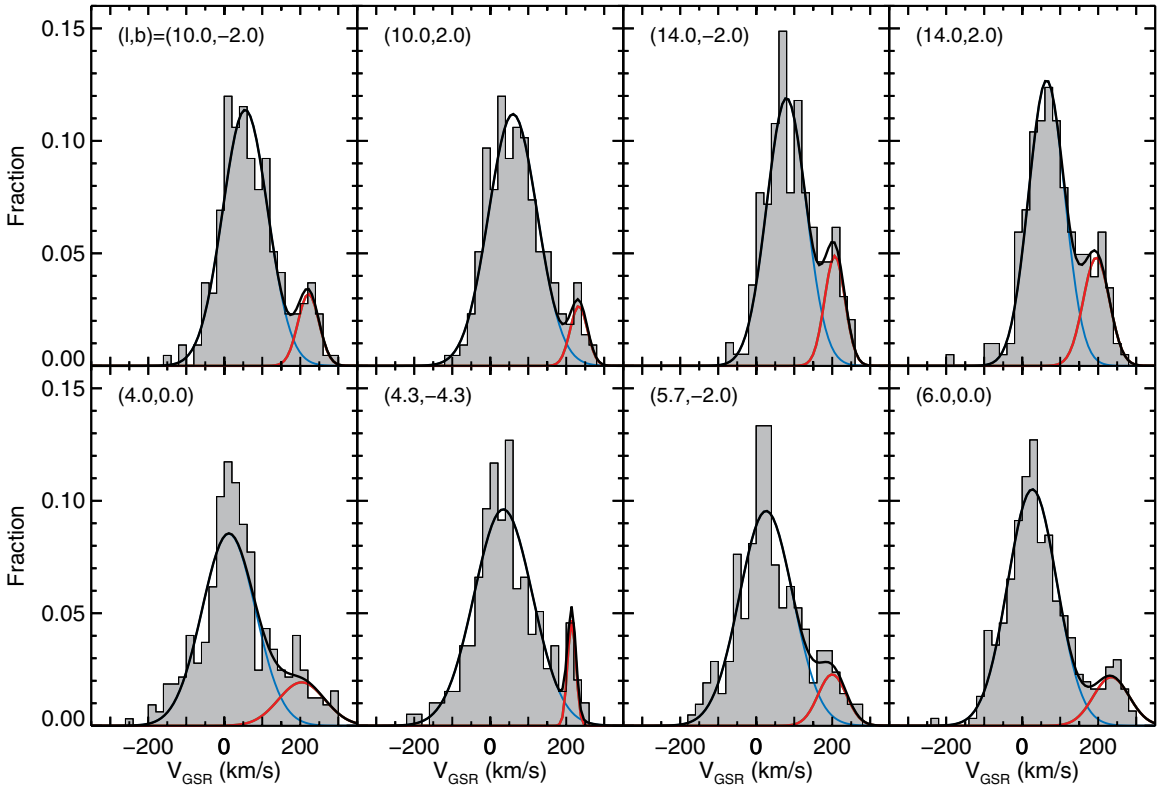

Figure 2. Velocity (V_{GSR}) histograms of eight APOGEE bulge fields showing a dual-peak structure, using 20 km s^{-1} binning. A two-Gaussian model (see the text) is fitted to the data to determine the central velocity of both peaks (blue/red lines). The solid black line is the sum of the two components.

(A color version of this figure is available in the online journal.)

3. RADIAL VELOCITY DISTRIBUTIONS: DATA AND MODELS

The bulge RV distributions exhibit a significant (and unexpected) number of high-velocity stars, which appear as prominent high-velocity peaks in eight fields and as high-velocity "shoulders" to the main peak in many of the other fields. We focus on the RV distributions of the eight APOGEE bulge fields with distinct high-velocity peaks, shown in Figure 2 with a $(J - K_s)_0 \geqslant 0.5$ selection. The stars in the high-RV peak account for ∼10% of the stars in a field. To derive the mean velocity of the high-velocity component, the histograms are fitted with a two-Gaussian model—a hot component for the bulge and a colder component for the high-velocity stars.[16]

These high-velocity peaks have not been previously detected in the MW bulge, including in the extensive BRAVA data ($-10^\circ < l < +10^\circ$, $b = -4^\circ, -6^\circ, -8^\circ$; Kunder et al. 2012). Several narrow peaks in the RV histogram were detected in the BRAVA data (Howard et al. 2008) but were eventually determined to be due to stochastic effects. Our high-velocity peaks are unlikely to be due to stochastic effects because (1) our sample per field is large (twice that of BRAVA), (2) the high-velocity peaks are seen in at least eight APOGEE fields, (3) the peaks appear at similar RVs following a general trend with longitude (Figure 3(a)), and (4) the pattern is "mirrored" across the midplane (e.g., strong similarities between $l, b = 10^\circ, \pm 2^\circ$). We conclude that the high-velocity peaks are due to real motions of stars in the Galaxy.

[16] The models are not intended to be perfect "physical" representations and are poor fits for several fields (e.g., [4.0, 0.0] and [5.7, −2.0]), but they serve well to estimate the peak center.

Table 1 gives the field name, longitude, latitude, diameter, mean V_{GSR} and velocity dispersion of all stars, number of stars, mean V_{GSR} of the high-velocity stars, the high-velocity threshold (essentially the velocity of the "trough" between the main and high-velocity peaks), and the number of high-velocity stars in the eight APOGEE bulge fields that exhibit the most distinct high-velocity peaks. To ascertain the nature of the high-velocity stars, we compare the APOGEE RV histograms to several models.

3.1. Besançon Galaxy Model

The Besançon Galaxy Model (Robin et al. 2003, 2012, hereafter BGM) simulates the stellar content in any given line of sight and computes the photometry, kinematics, and metallicity of each simulated star. For each population (thin disk, thick disk, halo, bar, and bulge), a star formation rate history, age, and initial mass function are assumed allowing the model to generate the distribution function of absolute magnitude, effective temperature, and age of the stars. Density functions are assumed for each population and tested against observations using photometric star counts. The model also includes a three-dimensional extinction map (Marshall et al. 2006) and simulated uncertainties on the observational parameters of each star.

The BGM bar and bulge populations are described in Robin et al. (2012). The bar is the more massive component and dominates the stellar content at low latitudes, while the bulge is longer and thicker and gives a contribution at intermediate latitudes where the bar becomes less prominent. The bar kinematics are taken from the Fux (1999) dynamical model, and the bulge kinematics are established to reproduce the BRAVA survey data (A. C. Robin et al., in preparation). This multi-population model also explains well the presence of double red

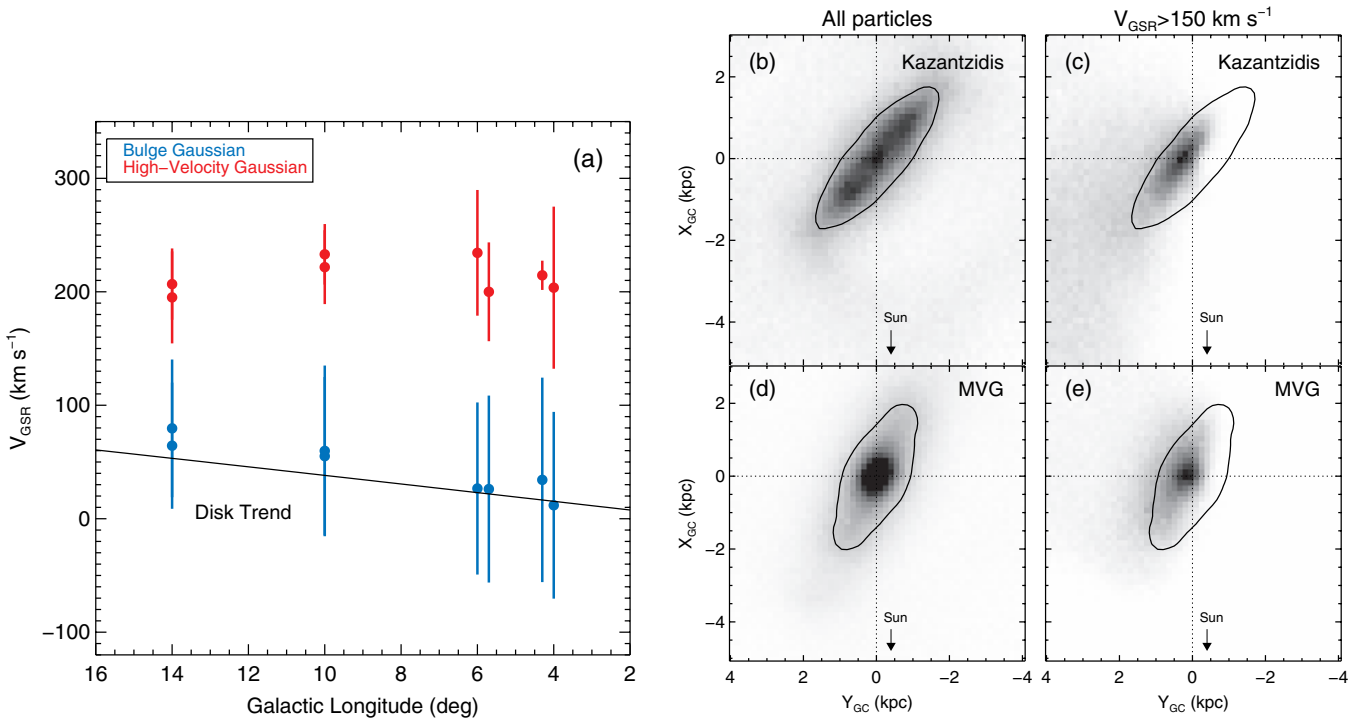

Figure 3. (a) Position–velocity diagram of the two-component Gaussian fits to the APOGEE bulge RV histograms, with main peaks in blue and high-velocity peaks in red. Gaussian FWHM values are indicated by the vertical lines. A general trend is seen in the high-velocity component, with mean velocity first rising with longitude and then slowly falling at longitudes above $l \approx 6°$–$7°$. The mean velocities of the main components fall close to the theoretical disk trend calculated from a simple rotation curve ($V_{GSR} = 220 \sin l$; black). (b–e) Spatial distribution of particles in the Kazantzidis 200 pc scale-height model (upper panels, b+c) and the MVG model (lower panels, d+e). All particles are shown in the left panels (b+d) while the right panels (c+e) show the distribution of particles with $V_{GSR} > 150$ km s^{-1} which live on the leading edge of the bar. The Sun's position is at (0,−8.5) which is off the lower edge of the panels. The black contours outline the general shape of the model MW bar.

(A color version of this figure is available in the online journal.)

Table 1
APOGEE Bulge Fields

Field Name	l_{cen} (deg)	b_{cen} (deg)	Diameter (deg)	$\langle V_{GSR} \rangle$ (km s^{-1})	σ_V (km s^{-1})	N$_{stars}$[a]	$\langle V_{GSR} \rangle_{high}$ (km s^{-1})	V_{thresh}[b] (km s^{-1})	N$_{high}$ (%)
004+00	4.0	0.0	1.0	39.4	100.9	376	203.6	141	56 (14.9)
004−04	4.3	−4.3	1.0	47.1	89.8	246	214.5	156	31 (12.6)
006−02	5.7	−2.0	1.0	39.5	88.4	245	200.0	146	29 (11.8)
006+00	6.0	0.0	1.0	50.2	96.1	364	234.3	177	39 (10.7)
010−02	10.0	−2.0	1.0	72.0	80.6	249	221.7	170	28 (11.2)
010+02	10.0	2.0	1.0	69.5	76.2	247	233.0	180	22 (8.9)
014−02	14.0	−2.0	2.0	93.7	77.3	247	206.8	176	32 (12.9)
014+02	14.0	2.0	2.0	85.2	85.2	251	195.1	171	36 (14.3)

Notes.
[a] Some fields have more than 300 stars due to multiple (distinct) plates being observed.
[b] The velocity threshold for the high-velocity stars.

clumps at medium latitudes (Nataf et al. 2010; McWilliam & Zoccali 2010; Saito et al. 2011) that are created by stars trapped in vertical resonances associated with the bar (e.g., Combes et al. 1990), lifting them to high altitudes.

3.2. Kazantzidis N-body Model

We also compare to the *N*-body model of Kazantzidis et al. (2008), which represents a MW-sized galaxy with an initial disk scale height of 200 pc. The model was subjected to a cosmologically motivated satellite accretion history and formed a bar as a consequence of the accretion events. The properties of the bar are similar to those of the MW bar (in overall orientation and size).

3.3. Martinez-Valpuesta & Gerhard Bar Model

The model developed in Martinez-Valpuesta & Gerhard (2011, hereafter MVG) is an *N*-body galaxy based on secular evolution of disk galaxies through angular momentum transfer between disk and halo. Once the bar appears, it grows stronger and buckles, forming a boxy bulge, such as the one seen in the MW. After this buckling the bar weakens and resumes growth by giving angular momentum to the live dark matter halo. At this point the bar has a short, thick component and a longer, thinner component. This model has already been quantitatively compared with the innermost region of the MW ($-8° < l < 8°$; Gerhard & Martinez-Valpuesta 2012) and also in the outer bar (Martinez-Valpuesta & Gerhard 2011) with good agreement.

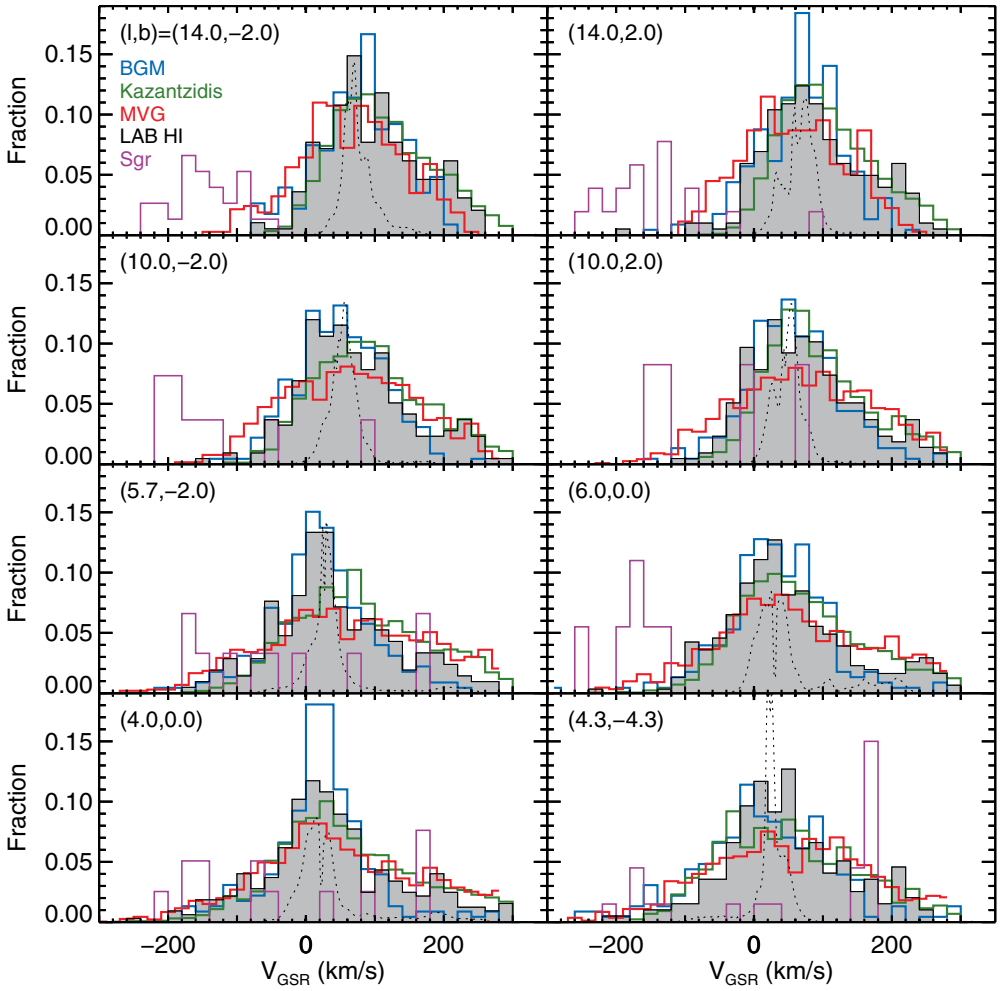

Figure 4. Velocity (V_{GSR}) histograms (fractions) of the APOGEE fields (black solid line and shaded region), compared to a variety of models and other data. The population synthesis "Besançon" model of Robin et al. (2003, 2012), which incorporates multiple kinematical prescriptions as described in Section 3.1 (BGM, blue). The *N*-body model of Kazantzidis et al. (2008) with an initial disk scale height of 200 pc as described in Section 3.2 (green). The *N*-body model of Martinez-Valpuesta & Gerhard (2011) as described in Section 3.3 (MVG, red). Integrated H I data within the field's FOV from the LAB survey (Kalberla et al. 2005, dotted black line scaled up by a factor of five). Predicted distribution of stars from the Sagittarius dSph streams, according to the model of Law & Majewski (2010, purple line scaled down by a factor of three). The Sagittarius model has been limited to points that could possibly fall within the APOGEE sample (i.e., we assumed all points had tip-RGB magnitudes, calculated their apparent magnitude, and removed all points too faint to be included in the sample).

(A color version of this figure is available in the online journal.)

3.4. Comparison to Models and Other Data

Figure 4 compares the observed APOGEE RV histograms (black solid lines and shaded region) to the above models.

The blue line shows one "observation" of the BGM, selected using the simulated photometric information and APOGEE targeting algorithms with model photometric errors and no reddening. The BGM reproduces the main features of most fields quite well, but not the high-velocity peak. Multiple simulated observations of the BGM were performed and found to be very similar, indicating that stochastic effects were small. Only one observation is shown for clarity.

The RV histograms of the Kazantzidis model are shown in green. This model cannot be mock "observed" like the BGM because synthetic photometry is not available. The RV distributions are a fairly good representation of the APOGEE histograms, but sometimes show a poorer match to the main RV peak, compared to the BGM. This model does show significantly more stars at high velocity and roughly match the fraction and distribution trend (decreasing number to even higher velocities) observed in the APOGEE data. However, it does not reproduce the "trough" between the main and high-velocity peaks seen in the APOGEE data.

The MVG model (red), as with the Kazantzidis models, reproduces the high-velocity stars much better than the BGM, although often "overpredicting" them. As in the Kazantzidis model, the MVG high-velocity stars are in the bar. This model also shows the interpeak "trough" in some of the fields (e.g., [14.0,−2.0], [6.0,0.0], and [4.0,0.0]).

The Leiden–Argentine–Bonn (LAB) H I data (Kalberla et al. 2005), shown as a dotted black line, display high-velocity peaks in some of the fields, but often at an RV different from the APOGEE peaks. Gas kinematics are complicated in the inner Galaxy but are dominated by forces influenced by the bar (e.g., Fux 1999). There does not appear to be a strong gaseous component of this new high-velocity stellar feature.

Finally, because the Sagittarius dwarf spheroidal galaxy (Sgr) and part of its tidal tails lie behind the bulge in this general direction, we test the APOGEE RVs against the recent Law & Majewski (2010) Sgr model (purple). It predicts very few Sgr particles in our fields and at RVs quite different from the APOGEE high-velocity peaks.

4. DISCUSSION

We detect high-velocity peaks in our APOGEE bulge RV distributions previously undetected in the data of BRAVA or any other survey; this might be due to the different regions sampled by the surveys (i.e., APOGEE probing lower $|b|$). We compare our stellar data to various models and H I data to discern the nature of this newly found "stellar population" of the bulge.

One potential explanation of this RV feature is that these stars are part of the tidal tail of Sgr, which lies close to the APOGEE bulge fields and has a mean velocity of $V_{GSR} \sim +170$ km s^{-1} at these longitudes (Law & Majewski 2010). However, initial distance estimates (using preliminary APOGEE stellar parameters and Girardi et al. 2002 isochrones) of ∼5–10 kpc for the APOGEE stars (also see isochrones in Figure 1(b)) make this explanation unlikely because Sgr and its tidal tails are ∼29 kpc distant (Siegel et al. 2011). In addition, the Law & Majewski (2010) model predicts very few high-velocity Sgr tidal tail stars in our fields (Figure 4).

Could these stars be a new substructure in the MW halo? We find this explanation unlikely because (1) the distribution of high-velocity stars in the dereddened color–magnitude diagram (Figure 1(b)) is almost identical to the rest of the stars in our fields (which should be dominated by the bulge/bar), with rough distances of ∼5–10 kpc, whereas a halo substructure should be more tightly clumped around one distance and metallicity; (2) the high-velocity stars constitute a large fraction (∼10%) of stars in the APOGEE fields, which is much larger than would be expected for halo substructure; and (3) the high-velocity stars are detected in many fields covering a large range of longitude, which would imply a truly enormous structure.

We therefore conclude that the high-RV stars are most likely members of the bar/bulge. Stars at these velocities and in comparable proportions of the total stellar population are predicted by the Kazantzidis and MVG *N*-body models; isolation and examination of these high-RV particles in the models reveal their membership in the Galactic bar. Furthermore, these model particles are grouped together on the "far" side (leading edge; see Figure 3(b)) of the bar, suggesting a coherent spatial/dynamical feature, rather than a sampling of stars with coincidentally similar velocities but on intrinsically unassociated orbits. (The lack of high-RV stars in the Besançon model may simply be due to their use of highly smoothed kinematical prescriptions.)

The nature and significance of the trough at intermediate velocities ($V_{GSR} \sim$ 140–180 km s^{-1}) is not clear. We have isolated the *N*-body particles occupying the RV trough but could not identify any group property, such as large distance, that would preferentially remove the corresponding stars from the APOGEE sample. It is possible that rather than an intrinsic trough (or drop in stellar surface density), the distribution is caused by an enhancement in phase space at high velocity from the combination of stars piling up at certain phases of their orbit (e.g., apogalacticon, Bureau & Athanassoula 1999) and projection effects. This explanation is supported by the structure seen in the fluid-dynamical model of Weiner & Sellwood (1999). In their Figures 6 and 8, a concentration of high-RV gas exists on the leading edge of the bar, with velocities and Galactic positions consistent with the high-RV particles "observed" in the Kazantzidis and MVG models. This concentration would correspond spatially with stars on x_2 orbits in the bar, perpendicular to the bar's major axis. In this scenario, the observed RV trough simply reflects the low count of stars at high RVs that are not in this dense dynamical structure. Why this property is not reproduced in the *N*-body models may be due to the resolution of the stellar structures contained within the model or the stellar density laws governing them.

The weight of evidence therefore suggests that the best explanation for the high-velocity stars is that they are members of the MW bar, grouped on particular orbits or phases of their orbit. The *N*-body models predict that high *negative* velocity stars should be seen at symmetrical longitudes in the fourth quadrant. Additional APOGEE data, follow-up data in the fourth quadrant, and future, more detailed model comparisons will yield insight into the nature of these features.

We thank Stelios Kazantzidis for giving us permission to use his *N*-body model. Support for D.L.N. was provided by SDSS-III/APOGEE and NSF grant AST-0807945. G.Z. was supported by a NASA Earth & Space Science Fellowship. A.C.R. acknowledges support from the French Agence Nationale de la Recherche under contract ANR-2010-BLAN-0508-01OTP. We thank the anonymous referee for useful comments that improved the manuscript.

Funding for SDSS-III has been provided by the Alfred P. Sloan Foundation, the Participating Institutions, the National Science Foundation, and the U.S. Department of Energy Office of Science. The SDSS-III Web site is http://www.sdss3.org/. SDSS-III is managed by the Astrophysical Research Consortium for the Participating Institutions of the SDSS-III Collaboration including the University of Arizona, the Brazilian Participation Group, Brookhaven National Laboratory, University of Cambridge, Carnegie Mellon University, University of Florida, the French Participation Group, the German Participation Group, Harvard University, the Instituto de Astrofisica de Canarias, the Michigan State/Notre Dame/JINA Participation Group, Johns Hopkins University, Lawrence Berkeley National Laboratory, Max Planck Institute for Astrophysics, Max Planck Institute for Extraterrestrial Physics, New Mexico State University, New York University, Ohio State University, Pennsylvania State University, University of Portsmouth, Princeton University, the Spanish Participation Group, University of Tokyo, University of Utah, Vanderbilt University, University of Virginia, University of Washington, and Yale University.

This publication makes use of data products from the *Wide-field Infrared Survey Explorer*, which is a joint project of the University of California, Los Angeles, and the Jet Propulsion Laboratory/California Institute of Technology, funded by the National Aeronautics and Space Administration.

REFERENCES

Benjamin, R. A., Churchwell, E., Babler, B. L., et al. 2005, ApJ, 630, L149
Binney, J., Gerhard, O. E., Stark, A. A., Bally, J., & Uchida, K. I. 1991, MNRAS, 252, 210
Blitz, L., & Spergel, D. N. 1991, ApJ, 379, 631
Bureau, M., & Athanassoula, E. 1999, ApJ, 522, 686
Bureau, M., & Athanassoula, E. 2005, ApJ, 626, 159
Chung, A., & Bureau, M. 2004, AJ, 127, 3192
Churchwell, E., Babler, B. L., Meade, M. R., et al. 2009, PASP, 121, 213
Cole, A. A., & Weinberg, M. D. 2002, ApJ, 574, L43
Combes, F., Debbasch, F., Friedli, D., & Pfenniger, D. 1990, A&A, 233, 82
Debattista, V. P., Mayer, L., Carollo, C. M., et al. 2006, ApJ, 645, 209
Dehnen, W. 2000, AJ, 119, 800
Dwek, E., Arendt, R. G., Hauser, M. G., et al. 1995, ApJ, 445, 716
Eisenstein, D. J., Weinberg, D. H., Agol, E., et al. 2011, AJ, 142, 72
Fux, R. 1999, A&A, 345, 787
Gerhard, O., & Martinez-Valpuesta, I. 2012, ApJ, 744, L8
Girardi, L., Bertelli, G., Bressan, A., et al. 2002, A&A, 391, 195
Gunn, J. E., Siegmund, W. A., Mannery, E. J., et al. 2006, AJ, 131, 2332
Gyuk, G. 1999, ApJ, 510, 205

Hammersley, P. L., Garzón, F., Mahoney, T. J., López-Corredoira, M., & Torres, M. A. P. 2000, MNRAS, 317, L45
Howard, C. D., Rich, R. M., Reitzel, D. B., et al. 2008, ApJ, 688, 1060
Kalberla, P. M. W., Burton, W. B., Hartmann, D., et al. 2005, A&A, 440, 775
Kazantzidis, S., Bullock, J. S., Zentner, A. R., Kravtsov, A. V., & Moustakas, L. A. 2008, ApJ, 688, 254
Kunder, A., Koch, A., Rich, R. M., et al. 2012, AJ, 143, 57
Law, D. R., & Majewski, S. R. 2010, ApJ, 714, 229
Liszt, H. S., & Burton, W. B. 1980, ApJ, 236, 779
López-Corredoira, M., Cabrera-Lavers, A., Mahoney, T. J., et al. 2007, AJ, 133, 154
Lütticke, R., Dettmar, R.-J., & Pohlen, M. 2000, A&AS, 145, 405
Majewski, S. R., Zasowski, G., & Nidever, D. L. 2011, ApJ, 739, 25
Marshall, D. J., Robin, A. C., Reylé, C., Schultheis, M., & Picaud, S. 2006, A&A, 453, 635
Martinez-Valpuesta, I., & Gerhard, O. 2011, ApJ, 734, L20
Martinez-Valpuesta, I., Shlosman, I., & Heller, C. 2006, ApJ, 637, 214
McWilliam, A., & Zoccali, M. 2010, ApJ, 724, 1491
Minchev, I., Nordhaus, J., & Quillen, A. C. 2007, ApJ, 664, L31
Nataf, D. M., Udalski, A., Gould, A., Fouque, P., & Stanek, K. Z. 2010, ApJ, 721, L28
Ness, M., & Freeman, K. 2012, in Assembling the Puzzle of the Milky Way, Le Grand-Bornand, France, ed. C. Reylé, A. Robin, & M. Schultheis, EPJ Web of Conferences, Vol. 19, 06003
Rattenbury, N. J., Mao, S., Sumi, T., & Smith, M. C. 2007, MNRAS, 378, 1064
Rich, R. M., Reitzel, D. B., Howard, C. D., & Zhao, H. 2007, ApJ, 658, L29
Robin, A. C., Marshall, D. J., Schultheis, M., & Reylé, C. 2012, A&A, 538, A106
Robin, A. C., Reylé, C., Derrière, S., & Picaud, S. 2003, A&A, 409, 523
Saito, R. K., Zoccali, M., McWilliam, A., et al. 2011, AJ, 142, 76
Siegel, M. H., Majewski, S. R., Law, D. R., et al. 2011, ApJ, 743, 20
Skrutskie, M. F., Cutri, R. M., Stiening, R., et al. 2006, AJ, 131, 1163
Weinberg, M. D. 1992, ApJ, 384, 81
Weiner, B. J., & Sellwood, J. A. 1999, ApJ, 524, 112
Wilson, J. C., Hearty, F., Skrutskie, M. F., et al. 2010, Proc. SPIE, 7735, 46
Wright, E. L., Eisenhardt, P. R. M., Mainzer, A. K., et al. 2010, AJ, 140, 1868